Available online at www.sciencedirect.com

SciVerse ScienceDirect

journal homepage: www.elsevier.com/locate/watres

Rapid field assessment of RO desalination of brackish agricultural drainage water

John Thompson [a], Anditya Rahardianto [a], Han Gu [a], Michal Uchymiak [a], Alex Bartman [a], Marcos Hedrick [b], David Lara [c], Jim Cooper [c], Jose Faria [c], Panagiotis D. Christofides [a], Yoram Cohen [a,*]

[a] Water Technology Research (WaTeR) Center, Chemical and Biomolecular Engineering Department, University of California, Los Angeles, CA 90095-1592, USA

[b] Panoche Drainage District, 52027 W. Althea Ave, Firebaugh, CA 93622, USA

[c] California Department of Water Resources, 3374 E. Shields Avenue, Fresno, CA 93726, USA

ARTICLE INFO

Article history:
Received 18 December 2012
Received in revised form
31 January 2013
Accepted 7 February 2013
Available online 4 March 2013

Keywords:
Agricultural drainage water
Brackish water
Desalination
Reverse osmosis
Mineral scaling

ABSTRACT

Rapid field evaluation of RO feed filtration requirements, selection of effective antiscalant type and dose, and estimation of suitable scale-free RO recovery level were demonstrated using a novel approach based on direct observation of mineral scaling and flux decline measurements, utilizing an automated Membrane Monitor (MeMo). The MeMo, operated in a stand-alone single-pass desalting mode, enabled rapid assessment of the adequacy of feed filtration by enabling direct observation of particulate deposition on the membrane surface. The diagnostic field study with RO feed water of high mineral scaling propensity revealed (via direct MeMo observation) that suspended particulates (even for feed water of turbidity <1 NTU) could serve as seeds for promoting surface crystal nucleation. With feed filtration optimized, a suitable maximum RO water recovery, with complete mineral scale suppression facilitated by an effective antiscalant dose, can be systematically and directly identified (via MeMo) in the field for a given feed water quality. Scale-free operating conditions, determined via standalone MeMo rapid diagnostic tests, were shown to be applicable to spiral-would RO system as validated via both flux decline measurements and ex-situ RO plant membrane scale monitoring. It was shown that the present approach is suitable for rapid field assessment of RO operability and it is particularly advantageous when evaluating water sources of composition that may vary both temporally and across the regions of interest.

1. Introduction

In recent years there has been an increasing use of reverse osmosis (RO) membrane technology for desalination of inland brackish sources, such as brackish groundwater and agricultural drainage water (Williams and Alemi, 2002; DWR, 2003; Greenlee et al., 2009; Lee et al., 2003; McCool et al., 2010; Mohsen et al., 2003; Sorour et al., 2003). High product water recovery is essential for inland water desalination in order to maximize water production while reducing the cost of brine management (Ahmed et al., 2001; Mohamed et al., 2005; Rahardianto et al., 2008). Product water recovery, however, is often limited due to high mineral scaling propensity associated with sparingly water soluble mineral salts such as

* Corresponding author. Tel.: +1 310 825 8766.
E-mail address: yoram@ucla.edu (Y. Cohen).

0043-1354/$ – see front matter © 2013 Elsevier Ltd. All rights reserved.
http://dx.doi.org/10.1016/j.watres.2013.02.013

gypsum ($CaSO_4 \cdot 2H_2O$), calcium carbonate ($CaCO_3$), barite ($BaSO_4$), as well as silica (SiO_2) (Boerlage et al., 2002; Braun et al., 2010; Drak et al., 2000; Hasson et al., 2001; Hoek et al., 2008; Semiat et al., 2003; Tran et al., 2007; Tzotzi et al., 2007; van de Lisdonk et al., 2001). Salt concentration increases axially along the RO membrane channel (being at a higher level at the membrane surface due to concentration polarization) and, with increased recovery, can exceed the solubility limit for sparingly soluble mineral salts. The level of salt supersaturation can be conveniently expressed in terms of its saturation index defined as $SI_x = IAP_x/K_{sp,x}$, where IAP_x and $K_{sp,x}$ are the ion activity and solubility products of mineral scalant x, respectively. When SI_x exceeds unity, mineral salt crystallization may occur in the bulk fluid and on the membrane surface (Rahardianto et al., 2008), leading to membrane mineral scaling, membrane surface blockage, loss of membrane productivity, as well as shortening of membrane useful life (Borden et al., 1987; Brusilovsky et al., 1992; Gilron and Hasson, 1987).

Mitigation of calcium carbonate scaling via pH adjustment (to acidic levels) is feasible since this salt's solubility increases with decreasing pH (McCool et al., 2010; Rahardianto et al., 2008). However, the solubilities of tenacious mineral salts such as gypsum, strontium sulfate and barite are relatively pH insensitive and thus antiscalant (AS) dosing of the RO feed has been widely practiced as a means of suppressing scaling by such salts (Ghafour, 2003; Neofotistou and Demadis, 2004; Shih et al., 2004; Tlili et al., 2003). Industry guidelines for effective AS use are based on RO operating conditions such that $SI_{CaCO_3} \leq 60$, $SI_{SrSO_4} \leq 8$, $SI_{CaSO_4} \leq 2.3–4$, $SI_{BaSO_4} \leq 60–80$, $SI_{SiO_2} \leq 1–3$ (Hydranautics, 2008; McCool et al., 2010).

Mitigation of membrane scaling using antiscalants requires appropriate AS selection and dose optimization (with respect to the specific water source, membrane type, target water recovery and operating conditions) in order to avoid: (a) overdosing (e.g., when scaling propensity decreases) that is both costly and may facilitate biofouling (Rahardianto et al., 2007; Vrouwenvelder et al., 2000), and (b) under-dosing (e.g., when water source scaling propensity rises) that can result in catastrophic membrane scaling. In addition, appropriate RO feed-filtration (with or without coagulation pretreatment) or other approach (e.g., air floatation) for removal of colloidal matter is needed to minimize RO membrane fouling by organics, microorganisms and colloidal matter and their potential negative impacts on RO operational and maintenance costs. In general, establishing effective RO feed filtration and mineral scale mitigation strategies require site-specific field testing (Alawadhi, 1997; Cohen, 2008).

Rapid field determination of the range of feasible RO operating conditions that addresses the range of needed feed filtration and AS treatment is clearly desirable, particularly in a single-pass mode of operation, since this is more practical. This is especially the case when confronted with the task of assessing source waters of varying quality from a multitude of geographical locations such as in the California's San Joaquin Valley (SJV) (McCool et al., 2010) which is the focus of the present study. In this region, which is one of the most productive agricultural regions in the United States (DWR, 2003), there are significant geographical and temporal water quality variations of groundwater and agricultural drainage water with regard to salinity and ionic composition, with total dissolved solids (TDS) in the range of 3000–30,000 mg/L (Lee et al., 2003; McCool et al., 2010). Therefore, cost-effective evaluation of the feasibility of RO desalting for the wide range of water source quality in the SJV would be best achieved through a rapid systematic field evaluation of RO feed treatment requirements and feasible product water recovery levels. Accordingly, the present study presents a novel approach to rapid field determination of the effective reverse osmosis (RO) desalting conditions for brackish water of high mineral scaling propensity.

The present approach focuses on the use of an automated small-scale Membrane Monitor (MeMo) (Bartman et al., 2010; Gu et al., 2013) for rapid field evaluation of RO desalting feed filtration requirements, optimization of AS treatment, and estimation of the RO water recovery level corresponding to the membrane scaling threshold. Accordingly, a field demonstration was conducted whereby, suitable RO operating conditions were derived using the MeMo system in single-pass mode of operation (i.e., no concentrate or permeate recycling), and subsequent tests were carried out with a mini-mobile-modular (M3) spiral-wound RO system (Gu et al., 2013). These latter field tests served to confirm the suitability of the MeMo identified operating conditions and where the MeMo was used as a scale detector for the M3 system.

2. Experimental

2.1. Reagents, materials and brackish water source

Desalination field tests were carried out with agricultural drainage (AD) water in the Panoche Water District of the San Joaquin Valley (Williams and Alemi, 2002; McCool et al., 2010; Smith, 1992). The source water was pumped directly from an underground sump (Drainage Site DP-25) and delivered to the RO systems (Sections 2.2 and 2.3). Grab samples of AD water feed were analyzed following standard methods by a state certified laboratory (Bryte Laboratory, Sacramento, CA) with the water quality data summarized in Table 1. It is noted that of the total dissolved solid content 14,400 mg/L about ~46% (6600 mg/L) consisted of sulfate with calcium concentration of 509 mg/L, thus making this water nearly saturated with respect to gypsum at $SI_g = 0.90$.

Membranes used in the RO pilot plant were spiral-wound elements (Dow FilmTec XLE-2540) each 6.35 cm (2.5 inches) in diameter and 101.6 cm (40 inches) long, with an active membrane area of 2.6 m^2 (~28 ft^2). These membrane elements were of average permeability of 4.57×10^{-3} $m^3/(m^2\text{-h-bar})$ and observed rejection of 97.7% (at 18.7 bar and 63% recovery for the water feed composition given in Table 1). Although the spiral-wound membrane system was typically used under safe (i.e., non-fouling, non-scaling) conditions, as established with prior MeMo diagnostic tests (Section 2.5), membrane cleaning was carried out when initiating a new series of tests or when specific scaling tests were conducted. Cleaning of M3 membrane elements was accomplished by periodically flushing the system with permeate or D.I. water, followed by cleaning with aqueous 0.1 wt% NaOH (pH ~12). When not in

Table 1 – Water quality data for the field study source water.

Raw feed water quality analysis	
Analyte	Reported value
Electrical conductance, μS/cm	14,810
Dissolved boron, mg/L	39
Dissolved calcium, mg/L	509
Dissolved chloride, mg/L	2650
Dissolved magnesium, mg/L	455
Dissolved nitrate, mg/L	597
Dissolved potassium, mg/L	7.6
Dissolved selenium, mg/L	1.7
Dissolved silica (SiO_2), mg/L	34.6
Dissolved sodium, mg/L	3890
Dissolved sulfate, mg/L	6660
pH	7.5
Dissolved hardness, mg/L as $CaCO_3$	3145
Total alkalinity, mg/L as $CaCO_3$	235
Total dissolved solids, mg/L	14,440

use, the spiral-wound membranes elements were stored in a preservative solution of 1 wt% sodium metabisulfite.

Flat-sheet membrane coupons used in the MeMo (membrane monitor) RO cell (Section 2.2), of the type used in the spiral-wound membrane, had active membrane area dimensions of 3.1 × 8.1 cm. Prior to use in the MeMo RO cell, each membrane coupon was first rinsed in DI water (for ~5 min) and subsequently stored submerged in DI water (for 1–2 h prior to testing). At the termination of each diagnostic test, membrane samples were analyzed via scanning electron microscopy with energy-dispersive X-ray spectroscopy (SEM-EDS) (JEOL JSM-6700F Field Emission SEM with EDS, Japan).

Two antiscalants were selected for scale suppression of gypsum, namely, Flocon 260 (BWA Water Additives, Tucker, Georgia) and PermaTreat PC-504T (Nalco Co., Naperville, Illinois), hereinafter referred to as AS1 and AS2, respectively. These antiscalants were previously evaluated to be suitable for scale suppression (Lyster et al., 2010; Shih et al., 2004).

2.2. *Mineral scale monitoring and diagnostic RO system*

Monitoring of membrane fouling and scaling was accomplished with an ex-situ membrane monitor (MeMo) (Fig. 1, (Bartman et al., 2010; Gu et al., 2013; Uchymiak et al., 2008)). Briefly, the MeMo system consisted of a high pressure transparent plate-and-frame reverse osmosis cell (feed channel dimensions of 3.1 cm wide, 8.1 cm long and 2.6 mm in height) suitable for operational pressures for both brackish and seawater desalting. The MeMo allowed for real-time membrane surface imaging (in the cell), as well as monitoring of permeate flux, feed flow rate, transmembrane pressure, as well as conductivity and temperature of feed and permeate streams. Feed, retentate, and permeate flow rates, along with temperature, pH, and conductivity of these streams were recorded digitally using a computerized data acquisition system described elsewhere (Gu et al., 2013). Feed to the MeMo, when operated in stand-alone mode, was provided via a partial stream from one of the two positive displacement pumps of the M3 RO pilot (Section 2.3). The MeMo feed was a sidestream from the tail RO element retentate when it was used as a process monitor for the RO plant. In this process monitoring mode, the MeMo operation was controlled by the integrated M3 control system. In both cases, feed to the MeMo was provided post M3 system filtration (Section 2.3) and the MeMo is operated in a single-pass mode. In the stand-alone mode, the MeMo feed flow rate and pressure were adjusted by a computer-controlled variable frequency drive (VFD) of the high pressure pump, a bypass valve before the RO cell and an actuated valve on the MeMo retentate line (located after the MeMo cell). In both operational modes, pressure and flow rates are adjusted via a specialized model-based controller for the system (Gu et al., 2013) in order to establish the desired level of concentration polarization (CP) in the MeMo RO cell. Results from previous hydrodynamics and mass transfer CFD modeling work, for this specific MeMo RO cell (Lyster et al., 2009), enabled precise characterization of the CP profile in the membrane channel for the range of operating conditions in the present study (cross flow velocity and feed pressure ranges of 4–8 cm/s and 1.0–2.8 MPa, respectively), and thus the level of solution supersaturation throughout the MeMo channel.

Lighting arrangement in the MeMo RO cell was set at a near dark-field condition in order to increase contrast for imaging of surface crystals. Surface imaging was with a high resolution CCD (charge-coupled device) camera attached to a monoscope that focused on the desired zone of the membrane coupon in the MeMo RO cell. In the present work, the monitored zone was a 1.0 cm × 1.3 cm area centered approximately a distance of 6 cm from the cell channel inlet. The entire membrane surface was also imaged by a high resolution digital camera. Membrane surface images were recorded at specified time intervals (typically 5 or 10 min) and analyzed online by specialized software (Bartman et al., 2010) to detect and quantify the percentage of the monitored area that was covered by particulate or other matter (including mineral scale), as well as the number density of mineral crystals. Given information on: (a) local level of solution supersaturation (at the membrane surface) at the imaged location, and (b) permeate flux and salt rejection, it is possible to establish the operating conditions (e.g., product water recovery, AS dose) at which mineral scaling/fouling would be expected to occur (or be averted) in a larger-scale RO desalting system (McCool et al., 2010). The premise of this approach is that SI_g in the MeMo membrane channel, at the observation zone, can be set (via control of the MeMo operation) so as to either match or be above or below the SI_g level expected in the monitored spiral-wound RO element of the plant (Sections 2.4 and 2.5, (Gu et al., 2013; McCool et al., 2010)). Finally, it is noted that once significantly scaled or fouled, the membrane in the MeMo was cleaned (online) with DI water or previously stored permeate water (Gu et al., 2013) or using standard cleaning protocols (Hydranautics, 2011) in order to restore the monitor to its original state (as verified by flux and rejection monitoring).

2.3. *M3 spiral-wound pilot RO system*

A mini-mobile-modular (M3) spiral-wound pilot RO system (Gu et al., 2013) was utilized for rapid field assessment of the optimal/feasible RO operating conditions. The M3 (Fig. 1)

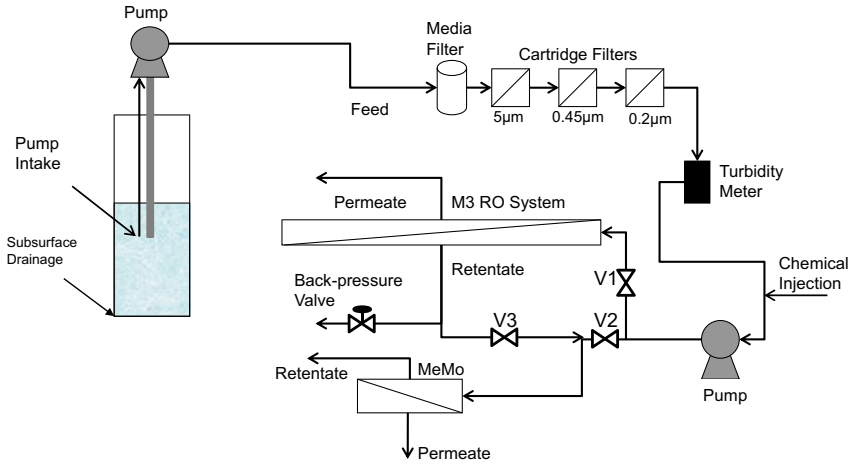

Fig. 1 – System setup for M3 and MeMo system operation. The initial filtration scheme (A) included only 5 μm and 0.45 μm cartridge filtration. The media filter and 0.2 μm cartridge filter were used only in the upgraded filtration scheme (Filtration scheme B). Valves V1, V2, and V3 were used to switch between the MeMo stand-alone and monitor modes.

consisted of the following modular unit operations: pretreatment, pumping, and RO desalting; each of which is connected to a central control system. In the present study, the M3 was loaded with six spiral-wound Dow FilmTec XLE-2540 elements with each element housed in a separate fiberglass pressure vessel (rated up to 68 bar). In the above configuration, the M3 was capable of permeate production of up to ~0.47 m^3/h (~3000 GPD) at 63% recovery for the field feed water source (14,440 mg/L TDS). The M3 filtration module (Filtration scheme A) contained a series of 5 and 0.45 μm filter cartridges (Keystone Filter, Hatfield, PA). Improvements in feed filtration (Filtration scheme B) in the field study were also evaluated with the addition of an auxiliary media filtration system that included a standard silica sand water filter (silver sand, US mesh #20, average sieve size 0.85 mm) as well as a 0.2 μm filter cartridge (Keystone Filter, Hatfield, PA). Once the source water was pre-filtered, it was fed to the RO plant via two positive-displacement high pressure pumps (Danfoss Model CM 3559, 3 HP, 3450 RPM, Baldor Reliance Motor, Danfoss Sea Recovery, Carson, California) controlled by variable frequency drives (VFDs) (Model FM50, TECO Fluxmaster, Round Rock, Texas). An electrically actuated needle valve (Model VA8V-7-0-10, ETI Systems, Carlsbad, California) on the retentate stream of the M3 RO system, along with the pump VFD, enabled control of the retentate flow rate and pressure in the RO unit using a model-based controller. Antiscalants, when employed, were injected into the feed water prior to RO desalting by using a metering pump (Model EHE31E1-V6, Walchem, Holliston, MA). Feed and retentate pressures were monitored using two pressure transducers (0–68 bar range, Model PX409-1.0KG10V, Omega, Stamford, Connecticut). Flow meters were installed on the feed, permeate, and retentate streams. A pH sensor (GF Signet Model 2750) and an inline turbidity meter (Micro TOL Model 20055, HF Scientific, Fort Myers, Florida) were installed at the RO feed (post-filtration) to monitor the feed pH and turbidity. Real-time data from all sensors were recorded via a computerized data acquisition system with all actuators (e.g., automatic valves and pump VFDs) under automated system control. Finally, it is noted that in normal M3 desalting, the MeMo system operated under the M3 control system (Fig. 1). In this configuration a concentrate side stream, from the tail element (6th element) of the M3 pilot, was fed to the MeMo RO cell in order to monitor for mineral scaling, which was expected to first occur in the M3 tail RO element.

2.4. *Estimation of recovery limits from MeMo field tests*

A relatively high CP level may be achieved in small plate-and-frame RO (PFRO) systems (Lyster et al., 2009; Uchymiak et al., 2008; McCool et al., 2010) even though these are operated at a low recovery (≤1–2%). Given knowledge of the salt concentration at the membrane surface, in the exit region of the PFRO RO cell (when operated in a single-pass mode and being fed with RO feed water), the equivalent recovery in a full-scale spiral-wound RO plant can be estimated for a specified acceptable level of concentration polarization (McCool et al., 2010). In this approach, surface salt concentrations at the MeMo membrane channel were first calculated, for the MeMo operating conditions using the numerical procedure developed specifically for the present RO cell geometry (Lyster et al., 2009). At the present level of analysis, the concentration polarization modulus, CP, (defined as $CP = C_M/C_B$ where C_B and C_M are salt concentrations in the bulk and at the membrane surface, respectively) was taken to be the same for all ions. Given the above information (at various locations on the membrane surface), mineral salt saturation indices and osmotic pressures for the feed and at various solution compositions (e.g., for different recovery levels) were then calculated using a multi-electrolyte thermodynamic simulation software (OLI, 2005). Subsequently, for the above MeMo solute concentration at the membrane surface (C_M), the acceptable operational ratio of C_M to the mixed cup retentate concentration, C_R (i.e., the average concentration of the retentate in the RO feed channel), in the tail element of the spiral-wound RO plant was estimated by introducing a CP allowance factor (i.e., $\alpha = C_M/C_R$). In practice, spiral-wound RO plants are

operated such that CP for an element is typically no greater than 1.2 (i.e., a CP allowance of 20% (Hydranautics, 2001b; McCool et al., 2010)). Since $\alpha <$ CP for a given operating condition, a conservative value of $\alpha = 1.1$ was selected to ensure that the practical limitation on CP was not exceeded. C_R can then be estimated for a given MeMo operation for which C_M is determined from knowledge of CP along the MeMo membrane surface.

Given the above, the equivalent recovery ($Y = Q_P/Q_f$, where Q_P and Q_f are the permeate and feed flow rates, respectively) for a spiral-wound RO plant can be obtained from McCool et al. (2010):

$$Y = \frac{1 - CF}{1 - CF - R_s} \quad (1)$$

where the retentate concentration factor is defined as $CF = C_R/C_f$ (McCool et al., 2010), C_f is the feed concentration, and the membrane salt rejection is given as $R_s = 1 - C_P/C_f$, where C_P is the permeate solute concentration. It is noted that CP for the RO plant tail element can be estimated as $CP_t = C_M/C_B = k \cdot \exp[2Y_t/(2 - Y_t)]$ (Hydranautics, 2001b), where Y_t is the recovery for the tail element, and k is an element-specific parameter (taken to be 0.98 for the present 40 inch long spiral wound elements). In the present work, flux from the tail element was monitored enabling estimation of CP_t and accordingly verifying that the system operation was within the recommended operational guidelines (Hydranautics, 2001b).

Prior to field determination of the recovery limits imposed by mineral scaling, the potential limits on recovery as imposed by the saturation indices for the sparingly soluble mineral salts (Section 1), were determined from information on the feed composition (Table 1) and using Eq. (1). The resulting saturation indices, based on the retentate mixed-cup concentration, for different recovery levels (Fig. 2) demonstrate that recovery would be limited due to gypsum scaling (i.e., $SI_g = 1$) to <10% and to just below 60% with the use of antiscalants (i.e., at $SI_g = 2.3$; (Hydranautics, 2008)). It is noted that calcite scaling has a lesser impact (Section 2.5) with saturation being reached at recovery of 0% and 72% at pH of 7.9 (or higher) and 6.5, respectively. The results in Fig. 2 provide an upper limit estimate of the recovery since $C_R < C_M$, while lower limits of recovery estimates would be obtained depending on the CP allowance (α) as depicted in Fig. 3. The above recovery estimates were subsequently assessed relative to field estimates based on the MeMo and operation of the spiral-wound RO pilot.

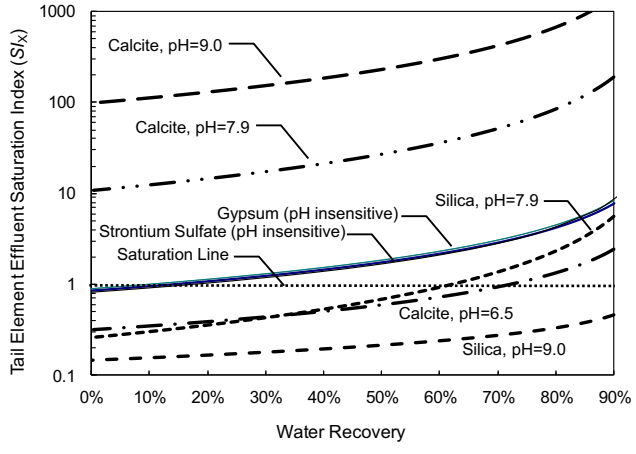

Fig. 2 – Variation of saturation indices for selected mineral scalants (gypsum, strontium sulfate, calcite, and silica) with product water recovery. Saturation is reached at SI = 1 indicated by the horizontal dashed line. Note: analysis was based on the water quality data given in Table 1.

2.5. *Rapid diagnostic field evaluation of RO operating conditions*

Field assessment of the suitable range of RO operating conditions was first carried out with the MeMo (in a stand-alone mode) in order to determine the necessary feed filtration, test AS performance and optimize its dose, and establish the maximum feasible recovery. The protocol for establishing the adequacy of RO feed filtration is depicted in Fig. 4. In this protocol the MeMo is initially operated in a stand-alone mode at a CP level that would be equivalent to RO plant operation at the recovery limit imposed by mineral scaling. This level is set to the mineral scaling threshold considering CP allowance of $\alpha = 1.1$; (Section 2.3, without AS feed dosing). The filtered feed is monitored to check if its turbidity is below the maximum recommended guidelines for RO feed (~1 NTU; (Hydranautics, 2001a)). The MeMo membrane surface is then monitored optically over a period of ~1–2 h. If the filtered feed turbidity is above the recommended level or if significant deposition of particulate matter or mineral crystals are observed on the MeMo membrane surface (even if the RO feed turbidity is <1 NTU), this would suggest needed feed filtration upgrade/improvement to further reduce the particulate concentration in the feed and thus its turbidity. The reason being that fine particulate matter, which deposits onto the membrane surface, can enhance nucleation of mineral salt crystals when the solution in the RO feed channel is supersaturated. Therefore, turbidity alone may be an insufficient indicator of the adequacy of feed filtration, hence the advantage of direct monitoring of the membrane surface in the MeMo RO cell.

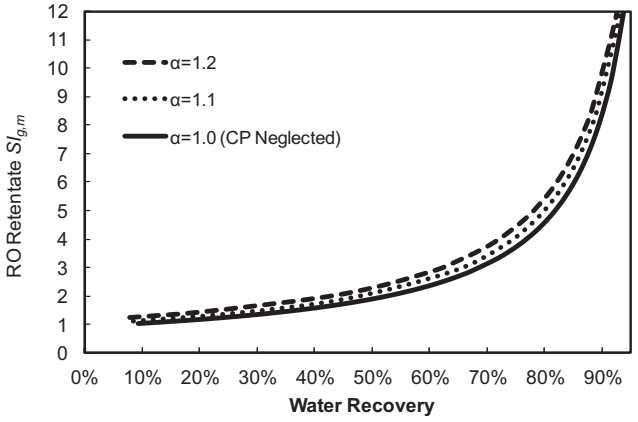

Fig. 3 – Variation of gypsum saturation index (SI_g) with product water recovery for RO desalting (based on the water quality given in Table 1) at various concentration polarization allowances.

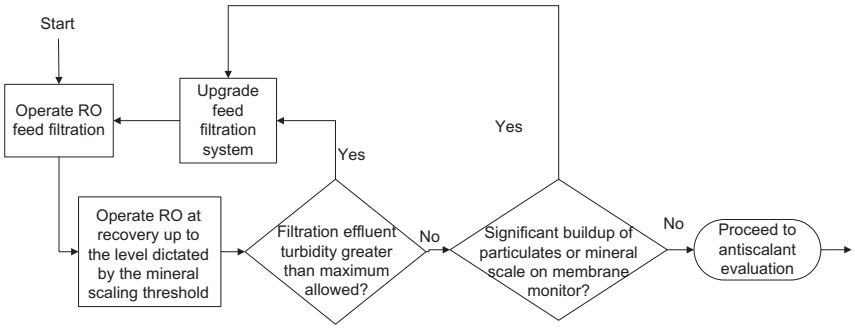

Fig. 4 – Protocol for evaluating the adequacy of feed filtration.

Once RO feed filtration is deemed adequate, one can proceed to assess the need for AS usage (delivered via a metering pump; Section 2.4) and AS selection and dose optimization (Fig. 5). In this experimental protocol, the MeMo operation is first set (by adjusting the crossflow velocity and transmembrane pressure) such that the saturation index at the membrane surface, for the scalant of concern (i.e., gypsum for the present water source), is elevated to a level corresponding to the desired recovery level (without AS addition). If mineral scaling is not detected (over a period of up to ~12 h) (Lyster et al., 2010), this would suggest that AS use is unnecessary for the set recovery level. However, if scaling is detected, or if it is desired to identify the maximum attainable recovery level with AS dosing, one can proceed with field comparison of scale suppression effectiveness (Fig. 5) for the selected pool of AS candidates. This evaluation should be done at a reasonable AS dose, via direct membrane surface observation with the MeMo system. AS dose is typically established on the basis of its scale suppression effectiveness at the desired recovery, with considerations of feed water chemistry and maximum manufacturer recommended level, as well as the impact of AS use on overall process economics.

The present water source (Table 1, Fig. 2) was supersaturated and nearly saturated with respect to calcite and gypsum, respectively. However, previous work has shown (Rahardianto et al., 2008) that calcium carbonate scaling is suppressed even under alkaline conditions (pH ~7–8) for feed water that is lean in carbonate and of high gypsum saturation when antiscalant is used for gypsum scale suppression. The attainable water recovery, with AS feed dosing, for the recommended bulk SI_g range of 2.3–4.0 (Hydranautics, 2008) (for the residual brine stream), as estimated via mineral solubility analysis (Section 2.4; Fig. 2), was expected to be in the range of 60%–77%. Accordingly, field evaluation of candidate antiscalants was carried out with the MeMo at an initial $SI_{g,m}$ of 3.1 at the membrane surface; this is about the average recommended limit for gypsum SI for its scale suppression by AS dosing (Hydranautics, 2008), which was equivalent to RO desalting of the present field water source at water recovery of 67%. Two candidate antiscalants (Section 2.1) were evaluated at a dose of up to 3 ppm. Once the more effective AS and its suitable dose were determined, the recovery limit imposed by mineral scaling was verified by operating the MeMo at incrementally increased levels of equivalent RO water recovery (Section 2.4) until detection of the onset of mineral scaling. Subsequently, validation of the selected operating conditions for set recovery limits, as determined via MeMo field tests, were carried out with the spiral-wound RO pilot (Section 2.3). In these field tests, the MeMo received a side stream of M3 concentrate from the tail RO element in order to monitor the onset of mineral scaling in the M3 plant. Mineral scaling detected in the MeMo was interpreted as an early warning of scaling occurring in the tail element of the M3, given that $SI_{g,m}$ in the MeMo was set at the same initial level as in the M3 tail element. Observed flux decline for the M3 tail element served as a confirmation of scale detection in the MeMo RO cell. The MeMo membrane was cleaned, after each discrete experiment, with either D.I. water or M3 RO permeate, which enabled effective removal of gypsum scale (Gu et al., 2013). Membrane coupons were replaced when scale removal by the above approach was ineffective.

3. Results and discussion

3.1. *Evaluation of feed filtration requirements for RO of agricultural drainage water*

Adequacy of the initial feed filtration system (5 and 0.45 micron cartridge filters; designated as Filtration A) was evaluated with the MeMo system in standalone mode, based on

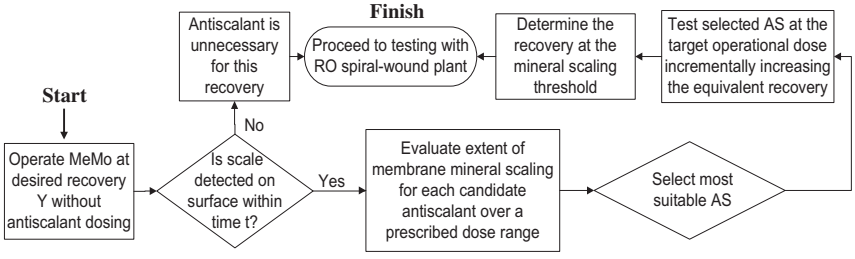

Fig. 5 – Field protocol for antiscalant selection and optimization protocol with the MeMo system.

short (60 min) desalting tests, without AS treatment, at an average surface $SI_{g,m}$ ~1.4 in the MeMo observation zone (27% equivalent recovery, $\alpha = 1.1$). During the above filtration tests, deposition of fine particulate matter was observed that rapidly covered the MeMo membrane surface (Fig. 6a, b) as is particularly noticeable in Fig. 6b. Significant permeate flux decline (~42% within 1 h) was also encountered (Fig. 7i) with about 80% membrane surface scale coverage at the MeMo observation zone (Fig. 6). Post analysis of the membrane (via SEM-EDS) indicated the presence of calcium sulfate precipitate, although previous mineral scaling studies have suggested that gypsum scaling should not be expected for the above gypsum saturation level until after ~5 h (Uchymiak et al., 2008; Rahardianto et al., 2008).

Given the high gypsum saturation in the raw feed water (SI_g ~0.90, Table 1), $SI_{g,m}$ was expected to exceed unity for recovery above ~10% (Figs. 2 and 3). Therefore, the effectiveness of AS treatment was first evaluated, via flux decline monitoring, for MeMo operation at $SI_{g,m} = 2.5$ (equivalent RO plant recovery of ~58% with $\alpha = 1.1$) with a reasonable 3 ppm dosage of AS1 as suggested in previous work (Kim et al., 2009; Lyster et al., 2010; Shih et al., 2004). Despite an increase in operational $SI_{g,m}$ from 1.4 to 2.5, flux decline was reduced to ~14% (Fig. 7ii), indicating partial suppression of mineral scaling by the added AS1. Nonetheless, the above level of AS1 dosing should have enabled scale free operation as reported for a similar water source (McCool et al., 2010). Therefore, it was surmised that insufficient filtration was likely the cause of the observed rapid fouling and contributor to enhanced scaling (due to seeding of crystals) even with reasonable AS dosing. Although Filtration scheme A (Fig. 1, Section 2.3) reduced feed water turbidity from ~6 NTU to ~0.5–1.0 NTU, cartridge filtration was observably insufficient for mitigating particulate deposition which is likely to have enhanced heterogeneous nucleation of mineral crystals (Cohen, 2008).

In order to improve feed filtration, a media filter was installed upstream of cartridge filtration and a 0.2 micron cartridge filter added just downstream of existing M3 filter cartridges (Fig. 1). With enhanced filtration B the filtered RO feed turbidity was reduced to <0.2 NTU. Although MeMo operation at initial $SI_{g,m}$ of 2.5 (equivalent to 58% RO plant recovery with $\alpha = 1.1$) without AS dosing did reveal a degree of scaling (Fig. 6c, d), there was significant reduction in the observed surface fouling in the MeMo test zone. Also, flux decline, relative to operation at the same $SI_{g,m}$ of 2.5 but with AS1 dosing, was somewhat lower for the test period of 1 h (Fig. 7iii). Upon AS1 dosing of 3 mg/L (also for MeMo operation at the above $SI_{g,m}$ level) mineral scale formation was effectively suppressed as indicated by the negligible flux decline in the short diagnostic test (Fig. 7iv). MeMo membrane surface imaging at a higher $SI_{g,m}$ of 3.1 (equivalent RO plant recovery of 67%) provided further confirmation that the upgraded filtration, along with AS dosing, were effective in suppressing mineral scaling (Fig. 8), with noticeable scaling occurring only after about 5 h of

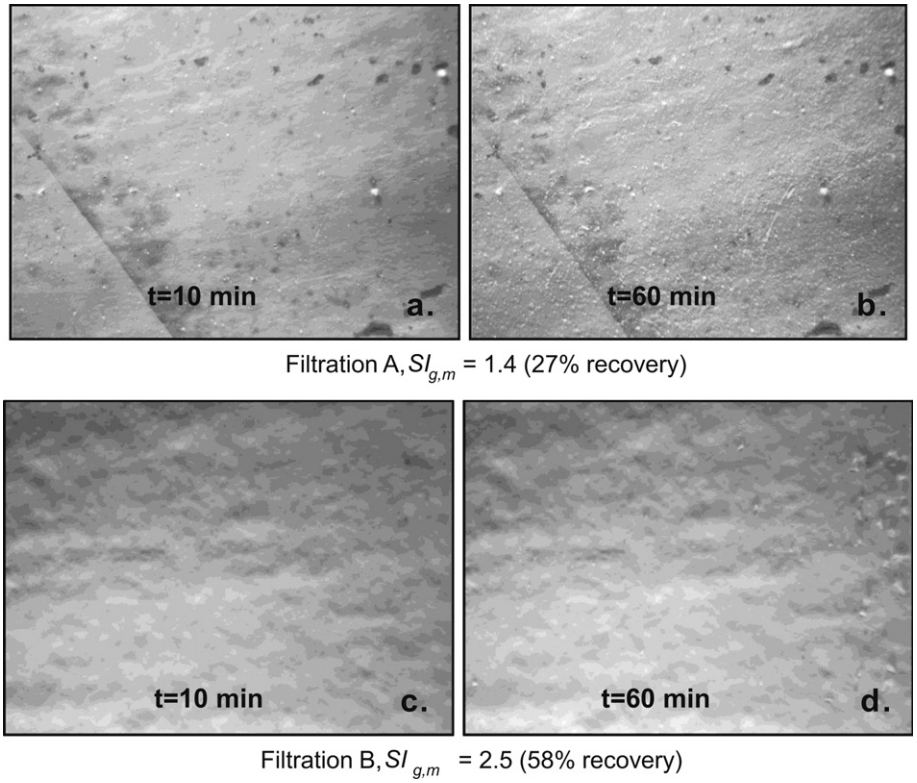

Fig. 6 – Membrane surface images of the MeMo observation zone for desalting of agricultural drainage water in a stand-alone operation. Images (a) and (b) are for operation at 27% equivalent recovery ($SI_{g,m} = 1.4$) with Filtration A (using a series of cartridge filters) without antiscalant dosing, at t = 10 min and 1 h, respectively, showing widespread particulate matter deposition observed in (a) and particularly in (b). Images (c) and (d) are for MeMo operation at 58% equivalent recovery ($SI_{g,m} = 2.5$) with upgraded Filtration B (media filtration and cartridge filters) without antiscalant treatment, showing a clean membrane surface (c), except for some initial mineral scaling on the right-hand region of (d). Observation area: 1.3 × 1.0 cm.

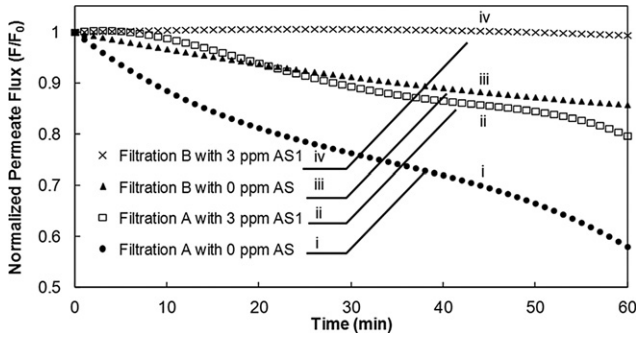

Fig. 7 – Permeate flux decline for MeMo tests of feed filtration adequacy for two different filtration schemes (Section 2.3). Filtration A (cartridge filters: 5 and 0.45 μm): i. Initial $SI_{g,m}$ = 1.4 (27% equivalent recovery) without AS dosing, and ii. $SI_{g,m}$ = 2.5 (58% equivalent recovery) with 3 mg/L dosing of antiscalant AS1. Filtration B: iii. Initial $SI_{g,m}$ = 2.5 (58% equivalent recovery) without antiscalant dosing, and iv. Initial $SI_{g,m}$ = 3.1 (67% equivalent recovery) with 3 mg/L dosing of antiscalant AS1.

operation. The above diagnostic tests suggest that suspended particulates (even for feed water of turbidity <1 NTU) in source feed water of high mineral scaling propensity could serve as seeds for promoting gypsum surface crystal nucleation. Therefore, for such water sources effective removal of suspended particulates is needed prior to RO desalting.

3.2. *Rapid antiscalant selection and dose optimization for mitigation of mineral scaling*

Final antiscalant selection and dose optimization were accomplished via a sequence of mineral scaling tests using the MeMo system post optimization of the feed filtration scheme (Section 2.2). Selection of the two candidate antiscalants, for field testing of scale suppression, was based on previously reported laboratory AS testing results (Kim et al., 2009; Rahardianto et al., 2008). Both antiscalants, AS1 and AS2, were compared at the same dose (3 mg/L) for the same initial $SI_{g,m}$ = 3.1 (in the observation zone), corresponding to an equivalent RO plant water recovery of 67% (for α = 1.1; see Section 2.4). Real-time membrane surface monitoring revealed that the evolution of surface mineral scale coverage on the RO membrane was significantly slower with AS2 than with AS1 as shown in Fig. 8. Scale coverage of about 44% was observed without AS use after 3 h, with 9% and 2% scale coverage after 10 h with AS1 and AS2, respectively, at the dose of 3 mg/L. Flux decline due to scaling (Fig. 9) was consistent with the observed surface coverage (at the same initial $SI_{g,m}$ = 3.1 for each antiscalant dosage). AS2 was more effective in delaying the onset of scaling (i.e., nucleation) and reducing the growth rate of gypsum crystals on the membrane surface, (i.e., retarding gypsum scaling), thereby resulting in fewer gypsum crystals on the membrane surface. Antiscalant feed dosing increased the observed scaling retardation time to ~1.5 h and ~8 h for AS2 dose of 1 mg/L and 2 mg/L, respectively, relative to 6 h for AS1 at 3 mg/L and only 20 min without AS use. AS2 was more effective in delaying the onset of mineral scaling, and at 3 mg/L dose reduced surface scale coverage (at the MeMo observation zone; Section 2.2) from ~45% to below 3% for the 10 h test (Figs. 8 and 10).

Although the above tests indicated that AS dosing at 3 mg/L was reasonable for operation of the RO plant at about 67% recovery, a more refined testing was undertaken (Fig. 10). In this test, the MeMo system was operated at successively increasing $SI_{g,m}$ (at the membrane surface in the observation zone) from ~1.9 to ~3.1 over a 45-h period (Fig. 10) with the equivalent recovery estimated based on α = 1.1 (see Fig. 3). Scale formation was first detected near the end of a 7-h MeMo desalting run at $SI_{g,m}$ of 2.9 (t = 25–32 h) representing an equivalent recovery of 64%. Upon increasing $SI_{g,m}$ to 3.1 (equivalent recovery of 67%, α = 1.1) during a subsequent 12-h

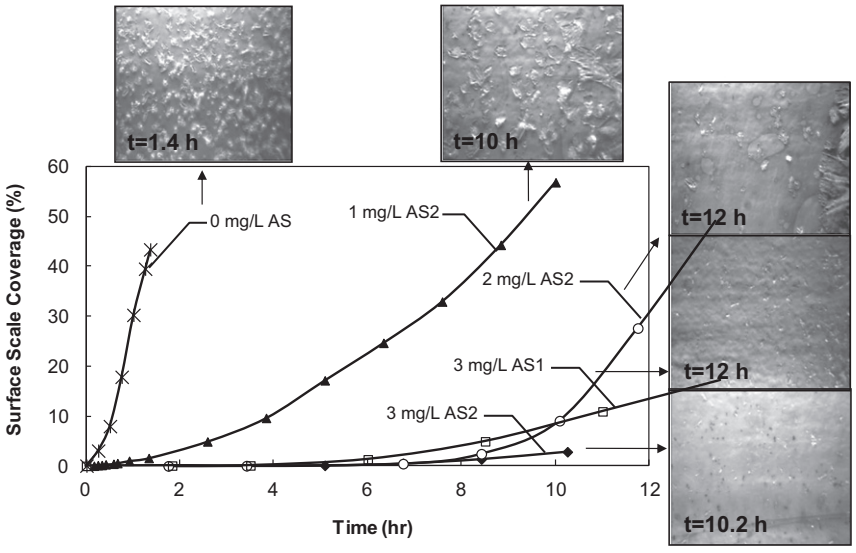

Fig. 8 – Evolution of the extent of gypsum scale coverage of the membrane surface in the MeMo observation zone for standalone MeMo operation at equivalent 67% recovery (initial $SI_{g,m}$ = 3.1) without antiscalant addition and which feed dosing with antiscalants AS1 (3 mg/L) and AS2 (1–3 mg/L).

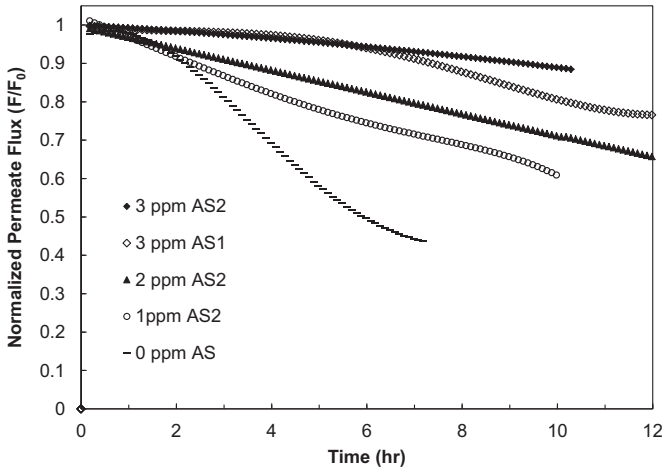

Fig. 9 – Permeate flux decline for field evaluation of antiscalant performance in a MeMo stand-alone operation corresponding to the scaling test conditions of Fig. 8. (Initial $SI_{g,m}$ = 3.1, all tests were conducted for the same initial flux, F_0).

period (t = 33–45 h), the appearance and growth of gypsum crystals on the membrane surface became more readily observable. The above gypsum supersaturation level was sufficiently high to overcome the AS2 capacity (at 3 mg/L dose) for suppression of gypsum crystallization. From the above results, it was reasonable to conclude that the membrane scaling threshold would be expected to be at an equivalent RO plant recovery of ~64% (assuming α = 1.1 and retentate $SI_{g,m}$ ~2.9).

3.3. *Field demonstration of AD water desalination with the M3 spiral-wound RO pilot*

In order to confirm the RO operating conditions identified as suitable for scale free operation in the diagnostic field testing (described in Sections 3.1 and 3.2), RO desalting was carried out with the spiral-wound M3 pilot system at a feed flow rate of 0.79 m^3/h with the MeMo installed for online scale detection (Fig. 1). The operational recovery range was 58–65%, producing permeate of salinity in the range of 370–400 mg/L total dissolved solids, for the set RO feed flow rate of 0.79 m^3/h. Initially, desalting was carried out at about 65% recovery ($SI_{g,m}$ ~3.0 at the exit region of the M3 tail element) (Section 2.4) with a low AS2 dosage of 0.5 mg/L. This test was undertaken, whereby operation of the MeMo was set such that $SI_{g,m}$ = 3.0 in the observation zone, in order to confirm the ability to monitor the onset and progress of scale formation in the RO plant. Mineral scaling was expected to occur (see Figs. 2 and 3) at the above operating condition, as was indeed verified by MeMo scale detection (Fig. 11). Mineral crystals were visually

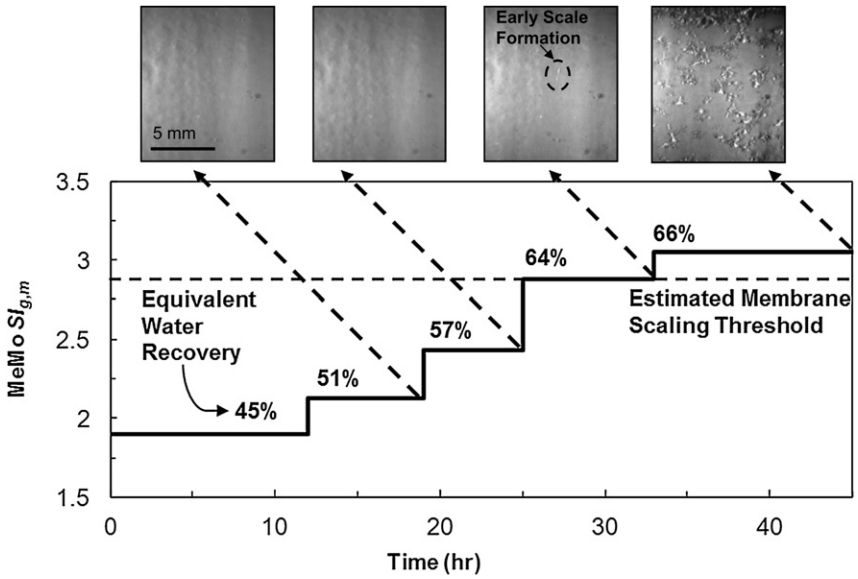

Fig. 10 – Field estimation of the mineral scaling threshold when the MeMo is operated at a standalone mode, with 3 mg/L feed dosing with antiscalant AS2, at different equivalent recovery levels of 45%, 51%, 57%, 64% and 66% corresponding to initial gypsum saturation at the membrane surface (in the MeMo observation zone) of 1.9, 2.1, 2.4, 2.9 and 3.1.

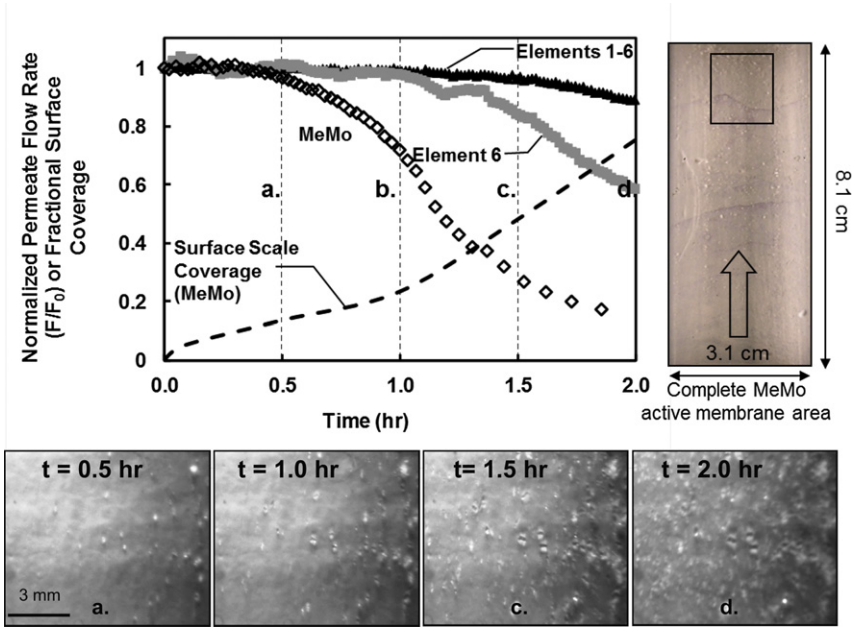

Fig. 11 – (Top) Normalized permeate flux for membrane elements 1–6 and for the tail element (element 6) of the M3 pilot for desalting operating at feed flow rate of 0.79 m^3/h and 65% recovery (tail element retentate initial $SI_{g,m} = 2.9$) with 0.5 ppm AS2 feed dosage. (Bottom) Membrane surface images from the MeMo observation zone set to operate with $SI_{g,m} = 2.9$ at the observation area. Initial overall and tail (6th) element permeate fluxes of 0.198 m/h (117 GFD) and 0.009 m/h (5.30 GFD), respectively. Right: entire membrane surface image ($t = 2$ h) reveals widespread mineral scaling that increases toward the RO channel exit (flow is in the arrow direction). Rectangle indicates the MeMo observation zone.

detected on the MeMo membrane (Fig. 11a, b) within the first 1 h of operation, prior to any significant measurable permeate flux decline either for the overall system (i.e., collective flux from M3 elements 1–6) or the M3 tail element (Fig. 11, Table 2). Indication of scaling could also be inferred from MeMo flux decline that reached about 20% within the first 0.5 h while there was no measurable change in flux detected for the M3 RO plant. MeMo flux declined progressively reaching 62% after 1 h, relative to only ~3% flux decline (within measurement uncertainty) for the M3 6th (i.e., tail) element (Table 2, Fig. 11). The above results indicated that monitoring RO plant flux decline did not provide sufficient sensitivity for early warning regarding membrane mineral scaling. Early detection of mineral scaling and its progression can, however, be quantified with the MeMo as a scale detector on the basis of membrane surface scale coverage (Fig. 11) and also by the number density of mineral crystals (in the MeMo observation zone). In principle, the first observed crystal in the MeMo could be considered as the earliest sign of the onset of mineral scaling. In the present study, in which images were captured every 5 min, the first instance of observed scale was as early as $t = 5$ min with the crystal number density (CND) being 40 crystals/cm^2 with a surface coverage of 1.1% of the detection zone (Table 2, Fig. 12). Clearly, the above would be a highly practical and sensitive test of the onset of mineral scaling.

Given the above validation of scale detection for the spiral-wound M3 plant operation, desalting with the M3 was then carried out with 3 mg/L AS2 dosing. The M3 plant was first operated at a safe recovery level of ~52% (Fig. 12). Subsequently desalting testing was increased to a recovery range of 60–64% (Fig. 12), just below the previously determined mineral scaling threshold (Figs. 2, 3 and 10, Section 3.2). At the above recovery range, it was determined that the RO tail element recovery was 8.8–10%, corresponding to a CP level in the tail

Table 2 – Operating conditions for test of RO pilot scale detection.[a]

Time (h)	Percent flux decline for the MeMo (initial $SI_{gm} = 2.9$)	Percent flux decline for the M3 RO tail element (initial $SI_{gm} = 2.9$)	Overall percent flux decline in the M3 RO system	Gypsum crystal number density (CND) in the MeMo observation zone (cm^{-2})	Mineral scale surface coverage (%) in the MeMo observation zone
0.5	20%	<1%	~0%	89	13
1.0	60%	1%	~0%	216	23
1.5	80%	10%	3%	523	48
2.0	>80%	39%	10%	820	75

a Test conditions and results are in reference to Fig. 11.

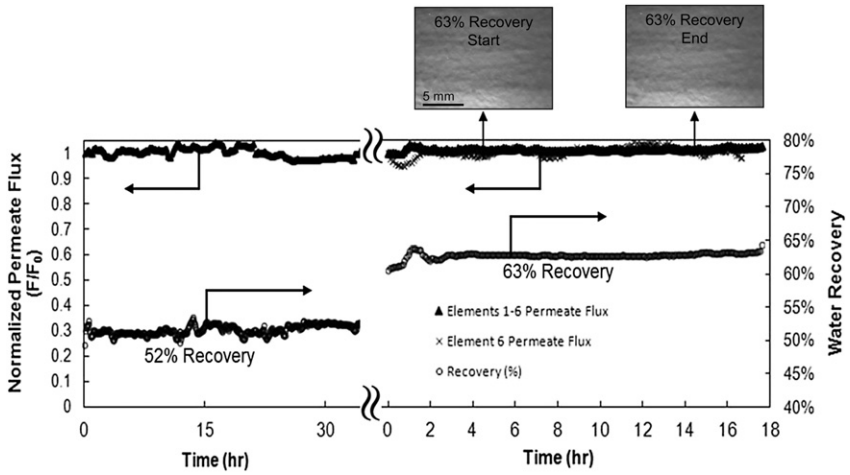

Fig. 12 – Product water recovery and permeate flux for M3 RO pilot field testing of AD water desalting at feed flow rate of 0.72 m^3/h (4500 gallons/day) with AS2 feed dosing of 3 mg/L. For 52% recovery: initial overall flux was 0.11 m/h (65.6 GFD). For 63% recovery: initial overall and 6th element permeate fluxes were 0.17 m/h (100 GFD) and 0.01 m/h (5.89 GFD), respectively. Initial, maximum and average recovery were 60%, 64% and 62.9%, respectively. MeMo operation was set at initial $SI_{g,m} = 2.8$ at the observation zone (equivalent RO plant recovery of 63%).

element of ~1.08–1.09, consistent with recommended industry guidelines and the present CP allowance (Section 2.4) used for estimating the attainable recovery based on MeMo diagnostic tests. The M3 plant was operated with the MeMo serving as an online monitor receiving a side stream from the last (i.e., 6th) element of the plant (Fig. 1). The MeMo was operated such that $SI_{g,m} = 2.9$ at the observation zone (equivalent to RO plant recovery of 64%). The RO plant operation was initiated at 60% recovery which was gradually increased up to a maximum of 64% for a short duration ($t = 1.0–1.5$ h). The recovery was then decreased and set to 63%, which was just below the mineral scaling threshold as ascertained in the stand-alone MeMo diagnostic tests (Fig. 10, Sections 2.5, 3.2). As expected, RO plant operation was scale free over the test period as indicated by both the lack of RO plant permeate flux decline and scale free membrane surface in the MeMo detection zone (Fig. 12). Overall, results of the study demonstrate the benefit of field deployment of the MeMo diagnostic system for establishing both suitable RO feed pre-treatment and RO operating conditions. Utilization of the online membrane fouling detection system would enable one to ensure safe RO operating conditions. Moreover, with appropriate interface of the MeMo system with RO plant control system, it should be possible to adjust plant operating conditions (e.g., feed flow rate, transmembrane pressure, antiscalant dosage) to aid in mitigation of fouling and mineral scaling.

4. Conclusions

- Rapid field evaluation of RO feed filtration requirements, selection of effective antiscalant type and dose, and estimation of suitable scale-free RO recovery level for a given source water can be achieved using a novel approach based on direct observation of mineral scaling and flux decline measurements, utilizing an automated Membrane Monitor (MeMo) that is field operated in a single-pass desalting mode.
- Suspended particulates (even for feed water of turbidity <1 NTU) in brackish source feed water of high mineral scaling propensity could serve as seeds for promoting surface crystal nucleation, as visualized via the MeMo system. Therefore, for such water sources effective removal of suspended particulates (beyond the typical recommended level for RO feed) is needed prior to RO desalting.
- A suitable maximum RO water recovery, with complete mineral scale suppression, achieved by a given antiscalant at a specific effective dose, can be systematically and directly identified, via the MeMo system, in the field for a given feed water quality.
- Scale-free operating conditions, determined via standalone MeMo rapid diagnostic tests, were shown to be applicable to a spiral-would RO system as validated via both flux decline measurements and ex-situ membrane mineral scale monitoring.
- The successful deployment of the present field diagnostic approach for assessing RO feed pretreatment and establishing suitable RO operating conditions, along with the positive benefit of online monitoring of membrane fouling merit evaluation of the current proposed methodology in long-term demonstration scale RO field study.

Acknowledgments

This work was supported, in part, by the California Department of Water Resources, the International Desalination Association, the U.S. Environmental Protection Agency, the California Desalination Coalition, and the U.S. Bureau of Reclamation. The authors also acknowledge support by Danfoss Sea Recovery for equipment contributions for construction of the M3 system, as well as antiscalants provided by BWA Water Additives and Nalco Company.

REFERENCES

Ahmed, M., Shayya, W.H., Hoey, D., Al-Handaly, J., 2001. Brine disposal from reverse osmosis desalination plants in Oman and the United Arab Emirates. Desalination 133, 135–147.

Alawadhi, A.A., 1997. Pretreatment plant design—key to a successful reverse osmosis desalination plant. Desalination 110 (1–2), 1–10.

Bartman, A.R., Lyster, E., Rallo, R., Christofides, P.D., Cohen, Y., 2010. Mineral scale monitoring for reverse osmosis desalination via real-time membrane surface image analysis. Desalination 273 (1), 64–71.

Boerlage, S., Kennedy, M.D., Bremere, I., Witkamp, G.J., Hoek, J.P.V.d., Schippers, J.C., 2002. The scaling potential of barium sulphate in reverse osmosis systems. Journal of Membrane Science 197, 251–268.

Borden, J., Gilron, J., Hasson, D., 1987. Analysis of RO flux decline due to membrane surface blockage. Desalination 66, 257–269.

Braun, G., Hater, W., zum Kolk, C., Dupoiron, C., Harrer, T., Götz, T., 2010. Investigation of silica scaling on reverse osmosis membranes. Desalination 250 (3), 982–984.

Brusilovsky, M., Borden, J., Hasson, D., 1992. Flux decline due to gypsum precipitation on RO membranes. Desalination 86, 187–222.

Cohen, Y., 2008. Membrane Desalination of Agricultural Drainage Water: Water Recovery Enhancement and Brine Minimization. University of California Water Resources Center, Riverside, CA.

Drak, A., Glucina, K., Busch, M., Hasson, D., Laine, J.-M., Semiat, R., 2000. Laboratory technique for predicting the scaling propensity of RO feed waters. Desalination 132, 233–242.

DWR, 2003. San Joaquin Valley Drainage Monitoring Program 2000. California Department of Water Resources, San Joaquin District.

Ghafour, E., 2003. Enhancing RO system performance utilizing antiscalants. Desalination 153, 149–153.

Gilron, J., Hasson, D., 1987. Calcium sulphate fouling of reverse osmosis membranes: flux decline mechanism. Chemical Engineering Science 42 (10), 2351–2360.

Greenlee, L.F., Lawler, D.F., Freeman, B.D., Marrot, B., Moulin, P., 2009. Reverse osmosis desalination: water sources, technology, and today's challenges. Water Research 43 (9), 2317–2348.

Gu, H., Bartman, A.R., Uchymiak, M., Christofides, P.D., Cohen, Y., 2013. Self-adaptive feed flow reversal operation of reverse osmosis desalination. Desalination 308, 63–72.

Hasson, D., Drak, A., Semiat, R., 2001. Inception of $CaSO_4$ scaling on RO membranes at various water recovery levels. Desalination 139, 73–81.

Hoek, E.M.V., Allred, J., Knoell, T., Jeong, B.-H., 2008. Modeling the effects of fouling on full-scale reverse osmosis processes. Journal of Membrane Science 314 (1–2), 33–49.

Hydranautics, 2008. Chemical Pretreatment of RO/NF. Technical Application Bulletin No. 111 Rev. C. http://www.membranes.com/docs/tab/TAB111.pdf.

Hydranautics, 2011. Foulants and Cleaning Procedures for Composite Polyamide RO Membrane Elements. Technical Service Bulletin 107.21. http://www.membranes.com/docs/tsb/tsb107.pdf.

Hydranautics, 2001a. Pretreatment: Membrane Fouling Considerations. http://membranes.com/docs/trc/pretreat.pdf.

Hydranautics, 2001b. Terms and Equations of Reverse Osmosis. http://www.membranes.com/docs/trc/termsequ.pdf.

Kim, M., Au, J., Rahardianto, A., Glater, J., Cohen, Y., Gerringer, F.W., Gabelich, C.J., 2009. Impact of conventional water treatment coagulants on mineral scaling in RO desalting of brackish water. Industrial and Engineering Chemistry Research 48 (6), 3126–3135.

Lee, R.-W., Glater, J., Cohen, Y., Martin, C., Kovac, K., Milobar, M.N., Bartel, D.W., 2003. Low-pressure RO membrane desalination of agricultural drainage water. Desalination 155 (2), 109–120.

Lyster, E., Au, J., Rallo, R., Giralt, F., Cohen, Y., 2009. Coupled 3-D hydrodynamics and mass transfer analysis of mineral scaling-induced flux decline in a laboratory plate-and-frame reverse osmosis membrane module. Journal of Membrane Science 339, 39–48.

Lyster, E., Kim, M.-m., Au, J., Cohen, Y., 2010. A method for evaluating antiscalant retardation of crystal nucleation and growth on RO membranes. Journal of Membrane Science 364, 122–131.

McCool, B.C., Rahardianto, A., Faria, J., Kovac, K., Lara, D., Cohen, Y., 2010. Feasibility of reverse osmosis desalination of brackish agricultural drainage water in the San Joaquin Valley. Desalination 261 (3), 240–250.

Mohamed, A.M.O., Maraqa, M., Handaly, J.A., 2005. Impact of land disposal of reject brine from desalination plants on soil and groundwater. Desalination 182, 411–433.

Mohsen, M.S., Jaber, J.O., Afonso, M.D., 2003. Desalination of brackish water by nanofiltration and reverse osmosis. Desalination 157 (1–3), 167.

Neofotistou, E., Demadis, K.D., 2004. Use of antiscalants for mitigation of silica (SiO_2)fouling and deposition: fundamentals and applications in desalination systems. Desalination 167, 257–272.

OLI, 2005. OLI Stream Analyzer 2.0. OLI Systems, Morris Plains, NJ.

Rahardianto, A., Gao, J.B., Gabelich, C.J., Williams, M.D., Cohen, Y., 2007. High recovery membrane desalting of low-salinity brackish water: integration of accelerated precipitation softening with membrane RO. Journal of Membrane Science 289, 123–137.

Rahardianto, A., McCool, B.C., Cohen, Y., 2008. Reverse osmosis desalting of inland brackish water of high gypsum scaling propensity: kinetics and mitigation of membrane mineral scaling. Environmental Science and Technology 42 (12), 4292–4297.

Semiat, R., Sutzkover, I., Hasson, D., 2003. Scaling of RO membranes from silica supersaturated solutions. Desalination 157, 169–191.

Shih, W.-Y., Albrecht, K., Glater, J., Cohen, Y., 2004. A dual-probe approach for evaluation of gypsum crystallization in response to antiscalant treatment. Desalination 169, 213–221.

Smith, B.E., 1992. Desalting and ground water management in the San Joaquin Valley, California. Desalination 87, 151–174.

Sorour, M.H., El Defrawy, N.M.H., Shaalan, H.F., 2003. Treatment of agricultural drainage water via lagoon/reverse osmosis system. Desalination 152 (1–3), 359–366.

Tlili, M.M., Manzola, A.S., Amor, M.B., 2003. Optimization of the preliminary treatment in a desalination plant by reverse osmosis. Desalination 156 (1–3), 69–78.

Tran, T., Bolto, B., Gray, S., Hoang, M., Ostarcevic, E., 2007. An autopsy study of a fouled reverse osmosis membrane element used in a brackish water treatment plant. Water Research 41 (17), 3915–3923.

Tzotzi, C., Pahiadaki, T., Yiantsios, S.G., Karabelas, A.J., Andritsos, N., 2007. A study of $CaCO_3$ scale formation and inhibition in RO and NF membrane processes. Journal of Membrane Science 296 (1–2), 171–184.

Uchymiak, M., Lyster, E., Glater, J., Cohen, Y., 2008. Kinetics of gypsum crystal growth on a reverse osmosis membrane. Journal of Membrane Science 314, 163–172.

van de Lisdonk, C.A.C., Rietman, B.M., Heijman, S.G.J., Sterk, G.R., Schippers, J.C., 2001. Prediction of supersaturation and monitoring of scaling in reverse osmosis and nanofiltration membrane systems. Desalination 138 (1–3), 259–270.

Vrouwenvelder, J.S., Manolarakis, S.A., Veenendaal, H.R., van der Kooij, D., 2000. Biofouling potential of chemicals used for scale control in RO and NF membranes. Desalination 132, 1–10.

Williams, C., Alemi, M., 2002. Agricultural Drainage in the San Joaquin Valley: a Gap Analysis, San Joaquin Valley Drainage Implementation Program. http://www.water.ca.gov/publications/.